Using Spectral Graph Wavelets to Analyze Large Power System Oscillation Modes

Lowery, Luke
Texas A&M University
lukel@tamu.edu

Baek, Jongoh
Texas A&M University
jongoh@tamu.edu

Birchfield, Adam
Texas A&M University
abirchfield@tamu.edu

Abstract

This paper presents a novel method for modal analysis to extract the spatial-temporal characteristics of oscillations in large electrical networks. A vector-fitted approximation of the Spectral Graph Wavelet Transformation (SGWT) and the inverse SGWT are derived to identify intra-network oscillations within a system response. This method scales linearly with the number of branches and leverages sparse solution techniques to develop a fast, low-memory estimation of modal frequency, shape, and damping. A case study on synthetic networks (2k-80k buses) with full dynamic modeling demonstrates consistent sub-second performance of modal estimation. Compared to existing methods, the SGWT approach can estimate modes with fewer channels and a shorter time-domain window. This presents a fast, general method for identifying true multiscale network behavior and localized oscillation sources, marking a novel application of graph-based signal processing.[1]

Keywords: multi-resolution analysis, modal analysis, spectral graph wavelets, oscillations, stability

1. Introduction

Monitoring low-frequency oscillations is an important aspect of power system stability. As a recent example, local and inter-area oscillations were observed in the half hour leading up to the 2025 Iberian grid blackout [7]. Undamped continued oscillations can cause hardware damage, fatigue, and outages. To ensure reliable service, operators seek to quickly identify harmful or potentially harmful oscillation modes and ensure they are sufficiently damped. Modal analysis of dynamic electrical networks serves to identify under-damped oscillation patterns within a grid.

However, the nonlinear nature of realistic generator models makes modal analysis non-trivial. With the increasing complexity of transmission and distribution networks, typical methods of modal analysis become increasingly difficult. For example, it is uncertain how the system response may evolve on different temporal and spatial scales in a large system with nonlinear components. Many popular methods also do not consider time localization, risking an oversimplification of the oscillation.

Beyond phasor-domain electromechanical oscillations, frequency-dependent EMT responses are becoming increasingly necessary to consider due to high-frequency power electronics. As generation develops in scope and complexity, the methods of modal analysis must be adapted in alignment with these modeling shifts.

Exciting developments in graph-based signal processing have prompted many novel publications in mathematics, signal processing, and numerical modeling over the past decade. This paper is the first application of Spectral Graph Wavelet Transformation (SGWT) to analyze the spatial nature of oscillations rigorously [5], significantly improving the analytical understanding of multiscale behavior over large transmission networks.

1.1. Literature Review

Many modal analysis techniques begin by considering a system response represented as a Hankel matrix, whose rows and columns index each signal and time sample, respectively. The time-domain response — obtained either empirically or through simulation — is then analyzed to obtain the prominent frequencies, damping, and pattern within the network.

Historically, most of these methods are a variation of *Prony's method*, a sum of time-domain exponentials with residues indicating each signal's participation in each mode. Modern methods such as Iterative Matrix Pencil (IMP) achieve this regression via singular value decomposition (SVD) [20]. Other methods, such as Dynamic Mode Decomposition (DMD) [2], also seek to

[1]To appear in the proceedings of the 2026 Hawaii International Conference on System Sciences.

find spatio-temporal oscillation modes. As the number of signals considered increases (i.e., large cases), these methods become victims of overfitting, often returning unrealistic or extraneous oscillation modes.

To mitigate these issues, some methods leverage temporal-wavelet analysis [4, 16] by accounting for temporal localization and the frame bounds of the response. The computational efficiency of the Continuous Wavelet Transformation (CWT) has improved significantly [1], often being preferred over Fourier-based methods. In many applications, the CWT is better equipped to analyze a windowed response in the time domain [14]. However, the CWT does not assist in identifying intra-network oscillation patterns (or *mode shape*).

There are also various methods of discovering oscillation modes through natural excitation of the system. These methods use either ambient or simulated data to estimate the impulse response of the system. The authors in [17] approximate the natural modes using a linearized system response from ambient PMU data.

Various graph signal processing (GSP) techniques exist that tackle time-domain graph signals, discussed in [13]. For example, the authors in [10, 9] use the Graph Fourier Transform (GFT), defining a Joint Fourier Transform (JFT) to study wave propagation over graphs. While some authors use Chebyshev approximations for numerical implementations (e.g. [12, 11]), some improvements can be made to improve scalability over sparse networks. The methods are not discussed in the context of electrical networks or mode identification. The authors in [15] propose a GFT technique based on the admittance Laplacian to analyze time-varying phasors, though the analytical foundation prompts more research.

Many open issues in GSP literature have implications for power systems. For example, non-static graphs (e.g., line outages and switching) are not currently well-suited for GSP analysis [13]. Additionally, a 'Fast GFT' (similar to that of the FFT) has yet to be developed, which is necessary to apply GSP methods reliably to large real-world models [18].

This review of state-of-the-art methods warrants research for novel methods of power-system modal identification within the GSP framework.

1.2. Novel Contributions

The paper's authors propose a novel graph-based technique to identify time-domain oscillations over large electrical networks as a function of scale, frequency, and bus localization. Unlike Prony-derived methods, the proposed SGWT framework passively encodes physical information at different spatial scales, making it ideal for mode shape identification. Through a novel vector-fitted approximation of the SGWT operator, this scalable method decomposes a system's frequency response into a domain where modal identification is simplified and has wave-like interpretations. Leveraging the recent developments in GSP, the authors develop a sparse framework to identify multiscale behavior over electrical networks.

2. Mathematical Preliminaries

The emerging field of graph-based signal processing using the *Graph Fourier Transform* (GFT) has enabled novel developments in mathematics, signal processing, and geometry processing in the past decade [18]. This section reviews the relevant foundation required to derive the proposed methods.

2.1. Graph Fourier Transform

Graph spectral theory characterizes an undirected graph $\mathcal{G}$ with n verticies and e edges by the arc-node incident matrix $\mathbf{A} \in \mathbb{R}^{e\times n}$ and the vector of branch weights $\mathbf{w} \in \mathbb{R}^e$. By extension, the graph Laplacian (sometimes *discrete Laplace-Beltrami operator*) can be defined in the vertex-domain (1) denoted by $\mathscr{L} \in \mathbb{R}^{n\times n}$.

$$\mathscr{L} := \mathbf{A}^T \text{diag}\,(\mathbf{w})\mathbf{A} \tag{1}$$

For a connected undirected graph, (1) is positive semi-definite (PSD) and guaranteed to have an eigenvalue decomposition $\mathbf{U}\Lambda\mathbf{U}^T$ and a real-valued spectrum. The existence of this decomposition allows the eigenvectors of (1) to be used to define a Fourier operator $\mathscr{F}$. For some function f over the network, let $\mathbf{f} \in \mathbb{C}^n$ represent the values of f at each vertex on the graph. Then, let the GFT operator (2) map the vertex-domain vector to its spectral form $\hat{\mathbf{f}} \in \mathbb{C}^n$

$$\hat{\mathbf{f}} := \mathscr{F}\mathbf{f} = \mathbf{U}^T\mathbf{f} \tag{2}$$

We introduce the notational practice of passing the graph Laplacian to a function as follows. By passing $\mathscr{L}$ as an argument to a vertex-domain function, this corresponds to evaluating $\hat{f}$ over the diagonal *spectrum* of the graph in the graph Fourier domain (3).

$$f(\mathscr{L}) \xrightarrow{\mathscr{F}} \hat{f}(\Lambda) \tag{3}$$

The convolution of two functions in the vertex-domain corresponds to a product of the two functions in the GFT-domain (4), similar to the temporal equivalent.

$$(f * g)(\mathscr{L}) \xrightarrow{\mathscr{F}} (\widehat{fg})(\Lambda) \tag{4}$$

Particularly relevant to the topic of the paper, the Fourier property of scaling holds in this domain (5). Observe that the Laplacian must be PSD for this relation to hold, which for (1) is guaranteed.

$$f\left(s^{-1}\mathscr{L}\right) \xrightarrow{\mathscr{F}} s\hat{f}\left(s\Lambda\right) \tag{5}$$

Moving forward, functions are implicitly in the vertex-domain, unless decorated by a hat (i.e., GFT domain).

2.2. Wavelengths on Graphs

In the context of this paper, the graph Laplacian is a generalization of the discrete second spatial derivative. For example, on the real line, this is approximated in a discrete context through central differences (6). This is an exact approximation in the instance of the parabola.

$$\nabla^2 f \approx \frac{f(x-h) - 2f(x) + f(x+h)}{h^2} \tag{6}$$

We generalize this approximation as a matrix operator with the graph Laplacian (1), when $\mathbf{A}$ is the forward difference operator (i.e., unscaled gradient) and branch weights are the squared inverse of h.

This observation extends to the general case of a graph with non-uniform branch distances. For each branch of length ℓ, the corresponding branch weight is ℓ^{-2}. Then the eigenvalues of the Laplacian represent the squared spatial frequency, which, when reordered, is precisely the wave equation (7).

$$(\nabla^2 - k^2)f = 0 \tag{7}$$

This implies that the spectrum of (1) is a discrete set of squared wavenumbers that map to principal waves on the graph (i.e., the eigenvectors), supported by the work in [8]. This is an informal statement of the *Spectral Theorem* [6]. From this point forward, the symbol $\mathscr{L}$ will be used to denote the graph Laplacian, as is common in GSP literature.

3. The Spectral Graph Wavelet Transformation

The wavelet transformation addresses some of the resolution issues of the Fourier transform. Without loss of generality, the eigenvectors of the GFT are global in the vertex domain. However, by localizing the spectral energy of a vertex-impulse (e.g., applying a smooth band-pass filter), a multiscale representation of the signal can be obtained that respects localizations in space [11].

In the following sections, the Dirac delta distribution (representing an impulse at a vertex) is used extensively. The distribution (8) is defined by a vector, mapping each bus to an indicator function that is only non-zero at bus n.

$$\delta_n(m) := \begin{cases} 1 & m = n \\ 0 & \text{otherwise} \end{cases} \tag{8}$$

A general overview of theory, application, scaling kernels, and admissibility criterion is reviewed in [11] in the context of the discrete SGWT.

3.1. The Wavelet Generating Kernel

The SGWT, at its core, is a smooth partitioning of the graph's spectra (perhaps a *strati-spectra*). The SGWT can be understood as a set of band-pass filters applied to the graph spectrum (Fig. 1). The unscaled filter, denoted by $\hat{\Psi}$, is referred to as the *wavelet generating kernel* or "mother wavelet". The resulting wavelets are simply the vertex-domain representations of this filter (9). In the vertex-domain, these filters can decompose a graph into localized perturbations for each graph scale (which represents wavelength in the context of this paper).

$$\Psi \xrightarrow{\mathscr{F}} \hat{\Psi} \tag{9}$$

These filters provide compact support in the vertex domain of the graph. By dilating the wavelet across the spectrum (Fig. 1), the vertex-domain wavelets are a spatially localized signal dilated to varying wavelengths.

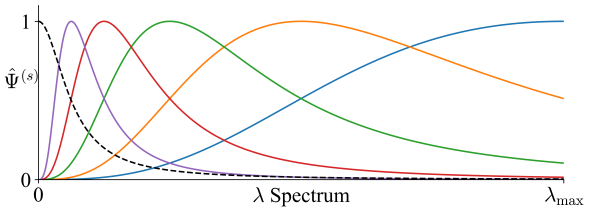

Figure 1. Wavelet (solid colors) and the scaling (dashed black) kernels in the graph spectral domain.

Scaled versions of the mother wavelet are denoted by $\Psi^{(s)}$, representing a spatial dilation by a positive scalar s per the scaling property of the GFT (5). The kernel $\hat{\Psi}$ is required to satisfy $\hat{\Psi}(0) = 0$ and all other criteria [11] to be admissible (i.e., valid).

To obtain a localized wavelet, a vertex impulse (8) is convolved with the wavelet kernel (10) using the convolution property of the GFT (4). A graph wavelet localized at bus n is denoted by Ψ_n, representing the

graph's response to the impulse across all possible spatial scales.

$$\Psi_n = \delta_n * \Psi \tag{10}$$

In the context of this paper, the scale represents changes in the wavelength, where a large s represents 'quasi-global' wavelets and a small s represents highly localized wavelets.

The *wavelet coefficients* (11) then describe ac-like components of a signal at each spatial scale s and at each bus n on the graph. The coefficients are scalars that describe how a signal appears *locally* in space. These are calculated via the inner product of each wavelet with a vertex-domain function $\mathbf{f}$. The wavelet coefficients matrix $\mathcal{W} \in \mathbb{R}^{n_b \times n_s}$ represents every permutation of vertex localization and scale, denoted by row and column index, respectively.

$$\mathcal{W}^{(s)} = \mathbf{f} * \Psi^{(s)} \tag{11}$$

Then, for some scale s, the coefficient vector $\mathcal{W}^{(s)}$ is a filtered version of $\mathbf{f}$ that retains ac-like behaviour over the graph at scale s. This is the core of the SGWT, decomposing a signal into spatial scales and vertex localizations.

3.2. Scale Discretizations

In practice, a discrete set of scales is used to perform the transformation – though the underlying kernels are continuous. The scales are typically chosen such that on a logarithmic scale, each scale of $\hat{\Psi}$ is evenly spaced (12).

$$s \in \{2^j : \lambda_{min} \leq 2^j \leq \lambda_{max}\} \tag{12}$$

where $\lambda_{min}, \lambda_{max}$ are the second smallest and the largest eigenvalue of the graph Laplacian, respectively.

The square root of each scale represents a bandwidth of the wavelengths over the graph. Furthermore, the wavenumber (spatial frequency) is roughly inversely proportional to the square root of the wavelet scale (13). This interpretation is supported by the ideas discussed in Section 2.2 via the wave equation.

$$k \approx \frac{1}{\sqrt{s}} \tag{13}$$

The scaled wavelet kernel $\Psi^{(s)}$ is often stored as a matrix, which is functionally a smoothed/filtered graph Laplacian. This calculates the wavelets for all vertex localizations concurrently when applied to a vector. This matrix can be obtained directly through spectral decomposition or through sparse methods discussed in Section 5.

3.3. The Inverse SGWT

The inverse transformation is used to reconstruct a signal from its wavelet coefficients. The full reconstruction of the signal requires the scaling coefficients to be computed along with the wavelet coefficients.

For brevity, we will assume that we are only interested in reconstructing intra-network oscillations (i.e., globally coherent oscillations are ignored). The wavelet portion of the continuous inverse transformation (14) has an affine relationship with the original signal. Let C_Ψ be the admissibility constant.

$$\mathbf{f} = \frac{1}{C_\Psi} \sum_n^{\mathcal{V}} \int_0^\infty \mathcal{W}_n \Psi_n \frac{ds}{s} \tag{14}$$

This can be evaluated in a discrete context by using log scales of s and a change of variable. Additionally, in the discrete context, the transformation needs to be scaled accordingly by the spacing between discrete scales (15).

$$C_\Psi = \frac{||\Psi||_\lambda^2}{\Delta \log(s)} \tag{15}$$

Then the discrete inverse can be expressed as a scale-weighted summation of the spectral wavelet functions (18) weighted by the wavelet coefficients.

4. Modal Analysis

This section applies the SGWT to identify oscillation modes from a time-domain system response. The following subsections detail the design choices used to implement the novel application in a scalable manner.

4.1. Joint Wavelet Transform

Similar to a JFT, a function of space and time can undergo a *Joint Wavelet Transformation* (JWT), where the time t and vertex n become parameters of the spectrum [10].

For each localization in space and time, the function is decomposed into its frequency ω and scale s components. The aggregate JWT (16) is a composite of the continuous temporal WT and the spectral graph WT. The joint wavelets can be interpreted as an approximate eigenfunction of the matrix pencil, except with a spatial-temporal localization.

The signal components (i.e., wavelet coefficients) of the transformation (16) are a function of the localizations, mapping space, time, frequency, and scale such that $\mathcal{W} : \mathbb{R}^4 \mapsto \mathbb{C}$. In a discrete context, this can

be expressed as a left and right transformation of the Hankel matrix of the signal.

$$\mathcal{W}^{(s,\omega)} = \Psi^{(s)}\mathbf{X}\Psi^{(\omega)} \tag{16}$$

A variety of procedures can be performed once this is obtained. The coefficients can be filtered, clustered, used for reconstruction, etc. Correlation techniques or energy methods can be used to determine temporal modes at different spatial scales.

4.2. Ring-Topology Example

This section provides the reader with a motivating example to visually communicate the physical interpretations of the proposed method. Consider a network that is configured in a ring-like loop (Fig. 2). This network is useful for demonstration, as the distance traveled can be parameterized trivially.

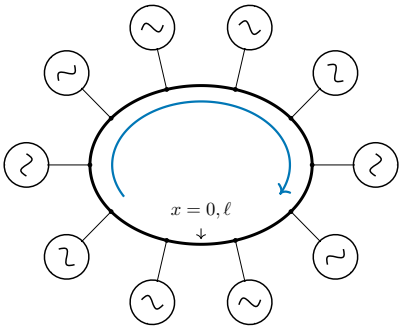

Figure 2. A topological one-line diagram of a ring-connected electrical network.

The example begins by performing an eigenvalue decomposition on the graph Laplacian (1). The resulting eigenvectors (Fig. 3) are the cyclic modes along the ring, where a small eigenvalue corresponds to a small wavenumber, and vice-versa.

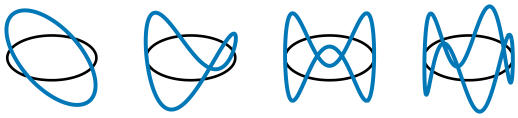

Figure 3. Four eigenvectors of the ring-bus system, representing physical modes rather than temporal modes.

These spatial frequency basis functions are used to construct the SGWT kernel, producing localized spatial wavelets. Using an admissible kernel, each wavelet can be computed at node n, representing an impulse δ_n at the respective node. An example of four discrete scales localized at the same vertex is shown in Fig. 4.

Figure 4. Spectral graph wavelets on a ring of buses, representing a localized spatial oscillation.

A contrived oscillation on the ring system (Fig. 5) contains a multiscale disturbance, with varying participation, duration, and frequency. The signal first undergoes both the fCWT and fSGWT independently. Then, when the joint coefficients are calculated via the JWT, the modes of the disturbance are clearly identified by local maxima in the spectral energy.

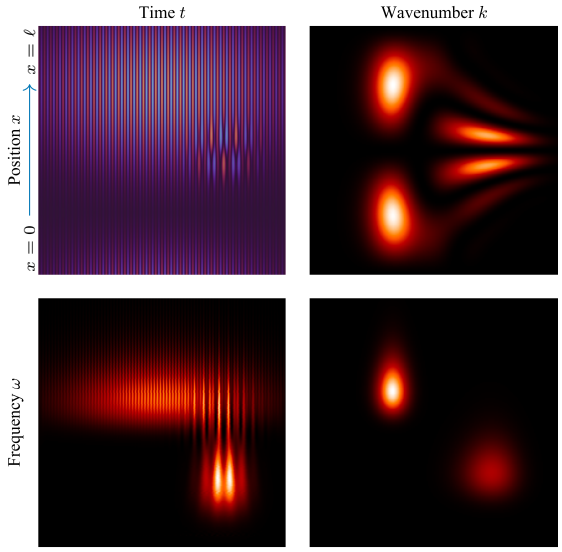

Figure 5. Spectrograms of a multiscale oscillation on the ring network (T-L) independently undergoes fSGWT (T-R) and the fCWT (B-L) when joined produce the JWT coefficients (B-R).

4.3. A SGWT Based Prony's Method

Once in the SGWT domain, a signal can be regressed to identify oscillations over the network at different spatial scales. By sampling localized coefficients at buses of interest, a smaller set of signals needs to be regressed to identify prominent modes.

Using a Prony-based method, the low-resolution system response can be decomposed into oscillation modes, which is significantly easier than analyzing the entire system response directly. In essence, the system response at bus n is decomposed into a discrete number of spatial resolutions (i.e., radial mode shapes) and regressed to approximate the temporal oscillations at each scale.

For each temporal mode in $\gamma \in \mathbb{C}^{n_\gamma}$, there is a corresponding vector of residues in the matrix $\mathbf{D} \in \mathbb{R}^{n_s \times n_\gamma}$ acting as weights for each spatial scale. The residues represent the components of the temporal oscillation on each *spatial scale* within the network.

$$\mathcal{W}_n(t) \approx \sum \mathbf{d}_\gamma^T e^{\gamma t} \tag{17}$$

Obtaining (17) is more efficient than regressing the Hankel matrix in its entirety. In addition to a smaller signal set, each coefficient scale 'embeds' information about the mode shape through the geometry of the wavelet in the vertex domain.

5. Implementation

The analytical derivation of the previous sections assumes that an eigenvalue decomposition is obtainable. For large systems, it is necessary to approximate the eigenvectors, as the generalized eigenvalue decomposition is not well-conditioned for networks with upwards of tens of thousands of nodes [11]. This section uses techniques from EMT numerical integration to derive a novel form of the Fast SGWT (fSGWT) ideal for sparse networks.

5.1. Vector Fitting the SGWT Kernel

Typically, a Chebyshev polynomial approximation is used to iteratively produce the wavelets with sufficient accuracy [19]. This paper demonstrates that a vector fit (VF) rational approximation of spectral graph wavelets is preferable for implementation.

Vector fitting is an unrivaled reduced-order modeling technique that is used to implement empirical, Laplace-domain functions in the time domain numerically. For example, in electromagnetic transient simulation, VF is used to regress propagation/admittance functions in the frequency domain, which can then be used to obtain practical time-domain solutions to convolution integrals of passive systems. In this paper, we instead use VF to approximate designed functions in the *spatial* frequency domain, to obtain practical bus/node/vertex domain functions.

Unlike Chebyshev polynomials, a VF approximation does not require the domain to be explicitly defined. Since the Chebyshev method is unstable outside its defined domain, a refitting is required if the graph connectivity or weightings are changed. Conversely, a VF model is defined on the entire real line (even though the graph Laplacian is PSD).

Furthermore, a VF model can obtain sufficient accuracy with a small order model, regardless of the graph's spectral width. This is valuable in large networks, as a Chebyshev approximation may require a higher-order model to approximate functions that scale logarithmically (such as the SGWT kernel).

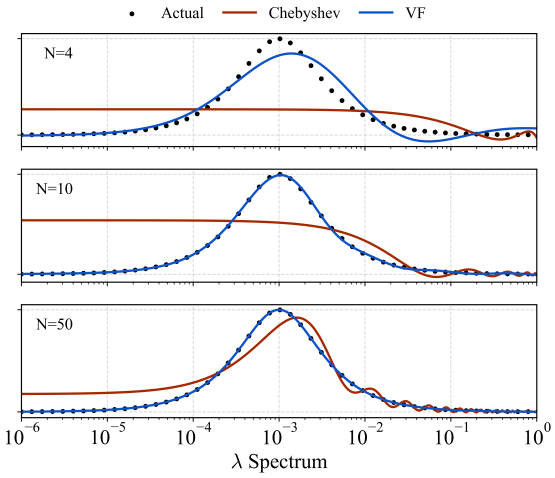

Figure 6. A one-dimensional comparison of a vector-fitted and Chebyshev-fitted kernel approximation.

The paramount advantage of VF is that each discrete wavelet scale (i.e., each filter) can be approximated with a common set of poles $\mathbf{q} \in \mathbb{R}^{\mathbf{n_q}}$. For each pole, a column in the residue matrix $\mathbf{R} \in \mathbb{R}^{n_s \times n_q}$ represents the individual contribution of each pole to each spatial scale.

$$\hat{\Psi}_\lambda \approx \sum \frac{\mathbf{r}_q^T}{\lambda + q} \tag{18}$$

In this context, each pole q is necessarily constrained to the real number line. The relative regression performance of the VF method compared to Chebyshev Polynomials is shown in Fig. 6. Performing VF for multiple scales (Fig. 7) is capable of reaching an approximation that requires fewer poles than the number of discrete scales.

We then use these residues and poles – which approximate a known frequency-domain function – to compute the vertex-domain wavelets for each scale.

This enables a scalable, sparse, and efficient framework for the SGWT.

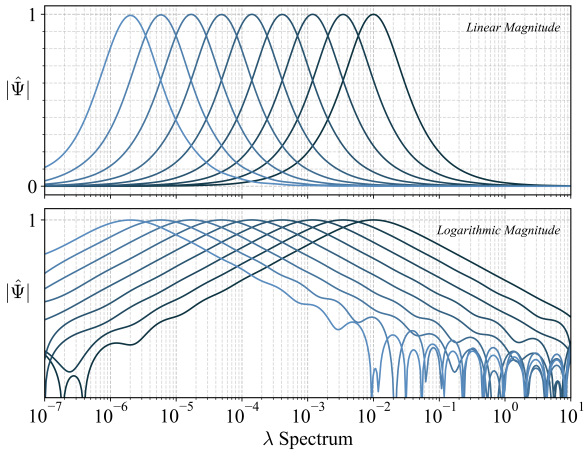

Figure 7. A VF approximation of the wavelet kernel for multiple scales, concurrently.

5.2. The Fast Spectral Graph Wavelet Transform

The orthodox fSGWT is based on the recurrence relation of Chebyshev polynomials. With a VF approximation, the wavelet transformation can be computed more efficiently. In the vertex-domain, the wavelet coefficients of the function $\mathbf{f}$ can be expressed as a sum of solutions to sparse linear systems (19). Solving via sparse Cholesky factorization is preferred, as transformations are assumed to be needed regularly. As $\mathscr{L} + qI$ is PD for all $q > 0$, a Cholesky factorization is guaranteed to exist. In fact, (19) is well-received by sparse solvers, with an abundance of functions to perform in-place factorization given a diagonal shift from a pre-factored matrix.

$$\mathcal{W} \approx \sum \left(\mathscr{L} + qI\right)^{-1} \mathbf{f}\mathbf{r}_q^T \tag{19}$$

The pseudo-code algorithm (Alg. 1) details the core operations performed in the proposed method. This procedure is identical for the scaling coefficients (spatial-dc). The time complexity after pre-factorization is $\mathcal{O}(n_q TE)$, scaling linearly with the number of poles, edges, and time samples, and theoretically independent of the number of scales.

Alternatively, (19) could be computed via recursive convolution, the rational equivalent of the distributed Chebyshev approach in [11].

Depending on the nature of the transformation, it can be more efficient to use this algorithm to generate and store the wavelets of each scale as a matrix. While this is preferable in some calculations, the sparsity of the computation is lost. Hence, the VF method is generally more efficient.

Algorithm 1: Fast Vector-Fit SGWT

Input: $\mathbf{f}$ Input signal
$\mathbf{L}$ Sparse Laplacian
$\mathbf{q}$ Poles
$\mathbf{R}$ Residues
Output: SGWT coefficients

```
fact = chol.prefactor(L)
for (q, r) ∈ (q, R) do
    fact.shift(q)
    W += fact.solve(f)r^⊤
return W
```

For instance, say we desire the SGWT coefficients for each scale s but are only interested in the localized coefficients at node n. Using the full SGWT (Alg. 1), the localized wavelet functions can be computed by passing δ_n (i.e., a vertex impulse) to the algorithm. This will be referred to as a *wavelet singleton*. Once each wavelet scale is obtained, the inner product of the singleton (Ψ_n) and the signal of interest (e.g., Hankel matrix) produces the wavelet coefficients localized at the specified vertex.

These coefficients are calculated efficiently over large networks since only one localization is considered. This sparse singleton transformation allows engineers to obtain localized wavelet coefficients on vast networks incredibly efficiently.

5.3. The Fast Inverse SGWT

Similar to the method used to approximate the SGWT (19), the vertex domain representation of the inverse can be solved as a summation of solutions to sparse linear systems (20). This can be derived by applying (19) to the definition of the inverse transformation (14).

$$\mathbf{f} \approx \frac{1}{C_\Psi} \sum (\mathscr{L} + qI)^{-1} \mathcal{W} \mathbf{r}_q \tag{20}$$

The implementation of the discrete inverse transformation (20) is only slightly different from the fSGWT implementation (Alg. 1), as they have nearly identical forms. To re-emphasize, the same poles and residues are used in both transformations.

This transformation can be used to decompress a signal, reconstruct a modal approximation, etc. As long

as the discrete scales are logarithmically spaced, the transformation is valid.

6. Results

This section provides the results, including assessing the preprocessing performance, a case study, and time complexity analysis of the proposed methods. The proposed methods are validated by using three different large synthetic grids (2k, 70k, and 80k bus [3]) as benchmark systems. The 70k and 80k bus cases are used to show the scalability of the method.

6.1. Design and Preprocessing

A continuous kernel design is provided to simplify the SGWT preprocessing procedure. Further, the kernel (21) is designed to make identification of peak spectral energy easy, such that s defines the maximum of $\hat{\Psi}^{(s)}$. A discrete number of logarithmically spaced scales is chosen, which should be selected to provide the desired spectral resolution. Then, the spectral-domain functions undergo vector fitting, and the residues and poles are stored for computation.

$$\hat{\Psi}(\lambda) = \left(\frac{\lambda}{1+\lambda^2}\right)^p \tag{21}$$

Next, the length-Laplacian of the network is computed and stored in a sparse matrix format. The inverse squared line length of each network branch (1) is used as a weight, and the buses are used as graph vertices. Transformers are assigned a distance of one to ten meters if not explicitly provided in the case data.

Samples of the vertex-domain wavelets generated for the 2k-Texas case are plotted in Fig. 8. Each sub-plot represents a different wavelength oscillation shape. These will be applied to the system response, acting as a 'mode shape filter' to identify buses that oscillate at a given frequency and distance.

6.2. Case Study

A benchmark contingency is simulated, and the bus frequency is recorded for modal analysis (Fig. 9). A generator at a substation in Bryan observes a three-phase bolted fault at $t = 1$s and is cleared at $t = 1.01$s. This contingency was chosen for the case study due to the presence of inter-area and local oscillations.

We start the analysis with the SGWT at a particular bus. The goal here is to determine the generalized 'width' or 'shape' of the oscillation quantitatively through the SGWT. Assessing the time-dependent SGWT coefficients (Fig. 10) allows the coherency of

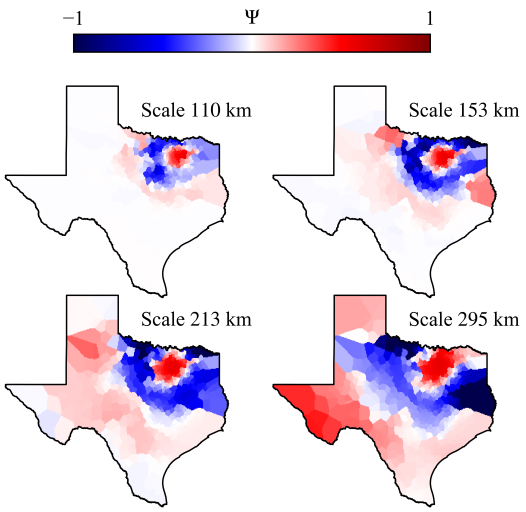

Figure 8. Spectral graph wavelets with varying spatial scale on the Texas 2000-Bus case, localized at the same node. These filters are then used to extract the mode shape from the system response.

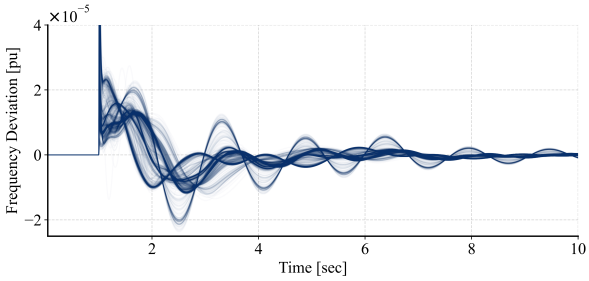

Figure 9. Benchmark frequency response of the Texas synthetic grid, caused by a three-phase bolted fault at a substation in Bryan.

the mode to be analyzed from the local reference frame of the bus.

The JWT coefficients (Fig. 11) are then computed using the fCWT on the signal in Fig. 10. For local coefficients, larger wavelength components represent perceived 'distant' relative oscillations, and the smaller wavelength components represent perceived 'local' relative oscillations. The analysis supports the claim that the oscillations at different spatial scales are identifiable by frequency, with a 0.3-0.4 Hz mode with a system-level wavelength of about 100 km, along with two perceived local modes.

While the singleton allows us to perform this calculation efficiently (see Section 6.3), it limits the available localizations to a single bus. For large systems, this can be a preferable trade-off, estimating

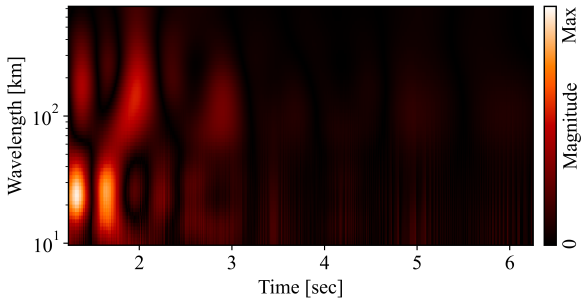

Figure 10. The time-dependent magnitude of the localized SGWT coefficients of the signal at the bus being studied.

the networks' oscillations via a localized approximation.

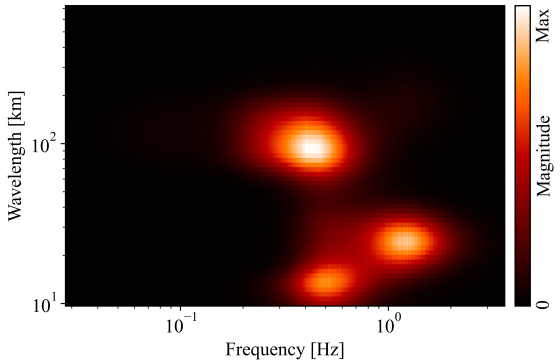

Figure 11. A scaleogram showing the magnitude of the JWT coefficients localized at one bus, integrated over time.

Using the full transformation, the shape of each mode can be extracted by the SGWT (Fig. 12), acting as a selective filter that retains signal features on the scale of inter-area oscillation modes. A wavelength of 300km is selected to study oscillations and mode shapes on this spatial scale. The 300km wavelet coefficients are calculated using the fSGWT algorithm, and the fCWT is performed and integrated over time to obtain an average spectrum.

6.3. Time Complexity

The time complexity is a significant advantage of the proposed method, with sparse SGWT methods scaling preferentially with the size of the sparse network. The run time to compute all wavelet coefficients (localizations and scales) for one sample in time is shown in Table 1. These times were obtained for a transformation with 65 discrete scales and a 25-pole

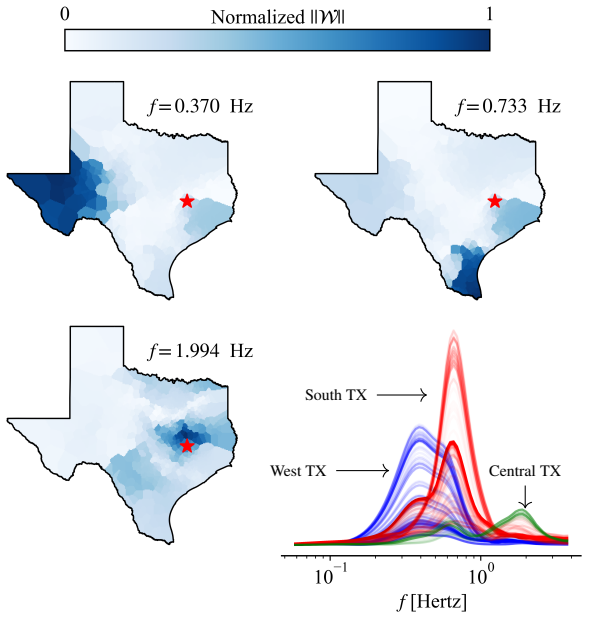

Figure 12. Mode shapes for three prominent frequencies quantified by SGWT wavelet coefficient magnitude, extracted with a wavelength of 300 km. The star indicates the location of the fault.

model. The algorithms were tested on a system with 80 GB of physical RAM and the following CPU specifications: 12th Gen Intel(R) Core(TM) i9-12900K, 3200 MHz, 16 Cores, 24 Logical Processors.

Table 1. fSGWT Performance with 65 scales

Case Name	fSGWT	iSGWT
NAEastWest80k	270 ms	330 ms
ACTIvSg70k	240 ms	280 ms
ACTIvSg2000	<7 ms	<7 ms

Using the same order model, a time-series response with 3k and 50k time points undergoes the singleton SGWT transformation (Table 2). The oscillation modes of the 80k bus system with 10s of simulation data can be approximated in less than one second. There is room for performance increase, as the majority of the runtime is dominated by the broadcasting of the singleton across the Hankel Matrix (a dense tensor product).

7. Conclusion

This paper established a preliminary graph-based wavelet framework to improve modal analysis. The vector-fitted SGWT kernel provides a fast method to perform spatiotemporal modal analysis over vast, sparse

Table 2. Singleton Time-Series Performance

Case Name	3k Time Steps	50k Time Steps
NAEastWest80k	<1 s	<7 s
ACTIvSg70k	<0.6 s	<5 s
ACTIvSg2000	<15 ms	<20 ms

networks. The proposed transformation successfully identifies localized network oscillations by leveraging the geometry of the system.

Future research should apply the proposed methods to forced oscillation source identification, as dissipating energy flow (DEF) can feasibly be calculated in the SGWT domain. Likewise, an assessment of the SGWT should be performed using online empirical data.

Furthermore, the wavelet transformation generally has some limitations compared to other modern transformations (i.e., contourlets, curvelets, shearlets). Therefore, we believe the application of so-called *Spectral Graph Shearlets* has the potential to improve modal identification.

This paper derives an application of the SGWT to obtain a physically informed wavelength representation of oscillation modes. With a novel VF implementation, the fSGWT approximates intra-network modes and is resilient to sparse sampling over the network. This scalable technique provides a fast and reusable modal analysis framework, identifying true multiscale behavior in large power systems.

References

[1] Arts, Lukas PA and Van den Broek, Egon L. "The fast continuous wavelet transformation (fCWT) for real-time, high-quality, noise-resistant time–frequency analysis". In: *Nature Computational Science* 2.1 (2022).

[2] Barocio, Emilio et al. "A Dynamic Mode Decomposition Framework for Global Power System Oscillation Analysis". In: *IEEE Trans. on Power Syst.* 30.6 (2015).

[3] Birchfield, Adam B. et al. "Grid Structural Characteristics as Validation Criteria for Synthetic Networks". In: *IEEE Trans. on Power Sys.* 32.4 (2017).

[4] Bronzini, M. et al. "Power system modal identification via wavelet analysis". In: *2007 IEEE Lausanne Power Tech*. 2007.

[5] Chen, Yunfei et al. "A Survey of Oscillation Localization Techniques in Power Systems". In: *IEEE Access* 13 (2025).

[6] Chung, Fan RK. *Spectral graph theory*. Vol. 92. American Mathematical Soc., 1997.

[7] ENTSO-e. "Iberian Peninsula Blackout". In: (May 2025).

[8] Girault, Benjamin. "Signal processing on graphs-contributions to an emerging field". PhD thesis. Ecole normale supérieure de lyon-ENS LYON, 2015.

[9] Grassi, Francesco, Perraudin, Nathanael, and Ricaud, Benjamin. "Tracking time-vertex propagation using dynamic graph wavelets". In: *2016 IEEE Global Conference on Signal and Information Process. (GlobalSIP)*. 2016.

[10] Grassi, Francesco et al. "A Time-Vertex Signal Processing Framework: Scalable Processing and Meaningful Representations for Time-Series on Graphs". In: *IEEE Transactions on Signal Processing* 66.3 (2018), pp. 817–829.

[11] Hammond, David K., Vandergheynst, Pierre, and Gribonval, Rémi. "Wavelets on graphs via spectral graph theory". In: *Applied and Computational Harmonic Analysis* 30.2 (2011). ISSN: 1063-5203.

[12] Leonardi, Nora and Van De Ville, Dimitri. "Tight Wavelet Frames on Multislice Graphs". In: *IEEE Trans. on Signal Processing* 61 (July 2013).

[13] Leus, Geert et al. "Graph signal processing: History, development, impact, and outlook". In: *IEEE Signal Processing Magazine* 40.4 (2023).

[14] Liccardo, Annalisa et al. "An Enhanced CWT-Based Approach for the Online Measurement of Low-Frequency Oscillations in Power Syst." In: *IEEE Trans. Instrum. Meas.* 73 (2024).

[15] Ramakrishna, Raksha and Scaglione, Anna. "Grid-Graph Signal Processing (Grid-GSP): A Graph Signal Processing Framework for the Power Grid". In: *IEEE Trans. on Signal Processing* 69 (2021), pp. 2725–2739.

[16] Rueda, José L, Juárez, Carlos A, and Erlich, István. "Wavelet-based analysis of power system low-frequency electromechanical oscillations". In: *IEEE Trans. on Power Syst.* 26.3 (2011).

[17] Seppänen, Janne M. et al. "Modal Analysis of Power Systems Through Natural Excitation Technique". In: *IEEE Trans. on Power Syst.* 29.4 (2014).

[18] Shuman, D. I. et al. "The emerging field of signal processing on graphs: Extending high-dimensional data analysis to networks and other irregular domains". In: *IEEE Signal Process. Mag.* 30.3 (May 2013). ISSN: 1053-5888.

[19] Shuman, David I, Vandergheynst, Pierre, and Frossard, Pascal. "Chebyshev polynomial approximation for distributed signal processing". In: *2011 Intl. Conf. on Distributed Computing in Sensor Systems and Workshops*.

[20] Trinh, Wei et al. "Iterative matrix pencil method for power system modal analysis". In: (2019).